Ordered structures of phthalocyanine overlayers on unpassivated InAs and InSb surfaces

2003 J. Phys.: Condens. Matter 15 S2631

(http://iopscience.iop.org/0953-8984/15/38/004)

INSTITUTE OF PHYSICS PUBLISHING JOURNAL OF PHYSICS: CONDENSED MATTER

J. Phys.: Condens. Matter **15** (2003) S2631–S2646 PII: S0953-8984(03)66046-7

Ordered structures of phthalocyanine overlayers on unpassivated InAs and InSb surfaces

S Yim and T S Jones

Centre for Electronic Materials and Devices, Department of Chemistry, Imperial College London, London SW7 2AZ, UK

E-mail: t.jones@imperial.ac.uk

Received 8 July 2003
Published 12 September 2003
Online at stacks.iop.org/JPhysCM/15/S2631

Abstract

The structure of copper phthalocyanine (CuPc) and free-base phthalocyanine (H_2Pc) overlayers deposited on the (001) and (111)A surfaces of InSb and InAs have been studied by low energy electron diffraction and van der Waals (vdW) intermolecular interaction energy calculations. CuPc forms a (3×3) structure on InSb(100) and a $(\sqrt{10} \times \sqrt{10})R \pm 18.4°$ structure on InAs(100). In contrast, H_2Pc forms a mixture of a (3×3) and $(\sqrt{10} \times \sqrt{10})R \pm 18.4°$ structure on InSb(100), whilst no ordered structures are formed when grown on InAs(100). These differences are rationalized by vdW intermolecular interaction energy calculations of the quadratic unit cells of CuPc and H_2Pc. For deposition on InSb(111)A, both molecules adopt a $(\sqrt{12} \times \sqrt{12})R30°$ structure. This energetically unfavourable hexagonal structure indicates a relatively strong substrate–molecule interaction. The lattice dimensions of the Pc unit cells deviate from that expected for a hexagonal Pc structure with an intermolecular interaction energy minimum.

1. Introduction

There has been considerable interest in the growth of ordered thin films of macrocyclic molecules for their application in a wide range of electronic and optoelectronic devices [1]. Phthalocyanines (Pcs) are a particularly important class of material, finding use, for example, in photovoltaic solar cells, organic light emitting diodes and field effect transistors [2–4]. This has led to a large number of studies aimed at understanding the growth and structure of Pc films on a wide range of substrate types.

From an energetic perspective, the surface overlayer structure of organic molecular thin films reflects the delicate balance of the intralayer energy associated with the interactions between molecules in the overlayer (E_{intra}), and the overlayer–substrate interface energy (E_{inter}). It is more precise to describe this energetic balance in terms of the relative magnitudes of the corresponding elastic constants, c_{intra} and c_{inter}, which are determined from the second

derivative, d^2E/dx^2, at the potential energy (PE) minima of E_{intra} and E_{inter} respectively, where x is a coordinate within the overlayer or along the overlayer–substrate interface [5].

The interfacial interaction with relatively inert substrates can be formed without any requirement for lattice-matching between dissimilar materials at the interface [1, 6]. For example, vapour deposition of organic molecules onto highly oriented pyrolytic graphite (HOPG) and layered materials such as MoS_2 frequently results in the formation of ordered thin films [7, 8]. However, in the case of a strong substrate–molecule interaction, for example with some metal and covalent semiconductor substrates, the actual structure of the molecular overlayer will reflect the competition between the energy lowering achieved by epitaxy, and the energetic penalty associated with any modification of the overlayer lattice from its native structure that may be required in order to achieve the epitaxy. There are a number of metal substrates on which weak chemisorption occurs and ordered films of intact molecules may grow. For example, epitaxial films of Pcs have been observed on single-crystal copper, gold and silver substrates [9, 10]. The ordered growth of organic molecules on inorganic semiconductor surfaces is however seldom achieved owing to the presence of chemically active dangling bonds at the semiconductor surface [11, 12]. Ordered organic thin films can be grown on these substrates if the dangling bonds are chemically passivated with some suitable species, such as H–Si(111) [13], Ag–Si(111) [37], Se–GaAs(100) [14] and Se–GaAs(111) [15]. Recently, however, there have been several reports of perylene-3,4,9,10-tetracarboxylic dianhydride (PTCDA) forming ordered layers on some unpassivated III–V semiconductor surfaces [16–18]. In this paper, we show that it is also possible to grow ordered overlayers of copper phthalocyanine (CuPc) and free-base phthalocyanine (H_2Pc) on several unpassivated InAs and InSb surfaces [19]. The formation of ordered structures suggests that the molecule–substrate interaction must be sufficiently weak to enable lateral diffusion of the molecules across the surface in order to achieve ordered films.

Attempts have been made to determine the surface structure and configuration of organic molecules using PE calculations. Calculations have been carried out on molecular layers formed on relatively inert substrates since the interfacial interactions are of the van der Waals (vdW) variety. For example, Forrest and Zhang [20] calculated the vdW PE of a PTCDA unit cell on a graphite substrate and proved that the structural parameters were consistent with scanning tunnelling microscopy (STM) and reflection high-energy electron diffraction (RHEED) results. More recently, the molecular arrangement of CuPc on H-terminated Si(001) has been determined by vdW PE calculations and compared with high-resolution frictional force microscopy results [21]. It is much more difficult to predict the structure of organic molecules on reactive inorganic semiconductor substrates since the force parameters of the substrate–molecule interaction are not known. However, most reports of ordered organic layers on inorganic semiconductors indicate commensurate epitaxy, suggesting that the elastic constant, c_{inter}, is quite large around the PE minima and the penalty associated with distortion of the bulk molecular configuration can be compensated. For commensurate structures, the overlayer molecules are all located on equivalent substrate sites. However, in the case of large organic molecules deposited on semiconductor substrates, the formation of several commensurate overlayer structures with similar unit cell dimensions is possible since the lattice dimensions of the substrates are usually much smaller than the unit cell dimensions of the molecular overlayer. The structure of a commensurate overlayer is likely to be determined by the intermolecular interaction energy since all the overlayer molecules lie simultaneously on symmetry equivalent substrate points. The interaction energy between the overlayer and the substrate is therefore the same.

In this paper we present examples of ordered structures (as viewed by low energy electron diffraction, LEED) of CuPc and H_2Pc deposited on several unpassivated III–V semiconductor

surfaces. Interestingly, the shape of the overlayer unit cells adopted is determined by the underlying substrate; in effect the substrate acts as a structural template. Quadratic Pc unit cells are formed on quadratic (100) substrates, whilst hexagonal Pc unit cells are adopted on hexagonal (111) substrates. Intermolecular interaction energies are calculated for quadratic and hexagonal unit cells of CuPc and H_2Pc, and the calculations provide a quantitative explanation for the different film structures formed.

2. Experimental details

The experiments were carried out in an ultra-high vacuum (UHV) system with a base pressure of $<4 \times 10^{-10}$ mbar. A microchannel plate LEED facility (Omicron) was used for collection of the diffraction patterns with a primary beam current of 0.1 nA. This low beam current allows for real time experiments of deposition with negligible beam induced damage. Low energy electron beam energies were used because of the large unit cells of the Pc overlayers. The InSb(100), InAs(100) and InSb(111)A substrates were cleaned *in situ*, after initial degassing at 250 °C for several hours, by two or three 15 min cycles of simultaneous argon ion bombardment and annealing (Ar^+ energies of 500 eV for InSb(100) and InAs(100) and 400 eV for InSb(111)A, substrate temperatures of 300, 225 and 275 °C respectively), followed by post-bombardment annealing to 300, 285 and 325 °C respectively for 20 min. Grazing incidence ions were used for the sputtering to reduce structural damage [22]. Further heating to 450–475 °C for InSb(100), 285–300 °C for InAs(100) and 400 °C for InSb(111)A was necessary to achieve the characteristic $(4 \times 2)/c(8 \times 2)$ LEED pattern for the (100) surface and the (2×2) diffraction pattern for the (111)A surface.

Commercially available CuPc (Aldrich, 97%) and H_2Pc (Syn Tech, 99%) powder was purified using temperature gradient vacuum sublimation. The purified organic molecules were then outgassed in the UHV system for 20 h before deposition, which involved sublimation from miniature Knudsen effusion cells. The substrates were held at room temperature and the amount of material deposited was calibrated using a quartz crystal microbalance (QCM) positioned near the substrate. Films grown at room temperature were annealed at various temperatures up to 300 °C for 30 min, the annealing temperature measured using a W–5% Re/W–26% Re thermocouple mounted on the manipulator in close proximity to the sample.

3. Theoretical details

Intermolecular interaction energy calculations were performed using a Lennard-Jones 9–6 vdW interaction energy for all possible, non-bonded atom pairs, i.e.,

$$E_{\mathrm{vdW(LJ\text{-}9\text{-}6)}} = \Sigma\varepsilon_{ij}\{2(R^*_{ij}/R_{ij})^9 - 3(R^*_{ij}/R_{ij})^6\} \tag{1}$$

where R_{ij} is the distance between the ith and jth atoms, R^*_{ij} is the minimum energy separation between atom i and atom j and $-\varepsilon_{ij}$ is the energy for the i, j interaction attained at $R_{ij} = R^*_{ij}$. Table 1 lists the molecular mechanics (MM) force field parameters for the Lennard-Jones 9–6 intermolecular interaction for the individual atoms in CuPc (figure 1(a)) and H_2Pc (figure 1(b)). The arithmetic mean of R^*_{ii} and R^*_{jj}, and the geometric mean of ε_{ii} and ε_{jj}, were used to express R^*_{ij} and ε_{ij}, the parameter values between the different types of atom, i and j. It is assumed that there is no significant contribution to the intermolecular interaction energy from Coulombic forces and higher-order multipoles, since previous calculations for non-polar molecules have shown this assumption to be generally valid [20, 21, 24].

CuPc [25] and H_2Pc [26] molecular structural parameter values, bond lengths and angles, obtained from *ab initio* methods and density functional theory (DFT) calculations were used for

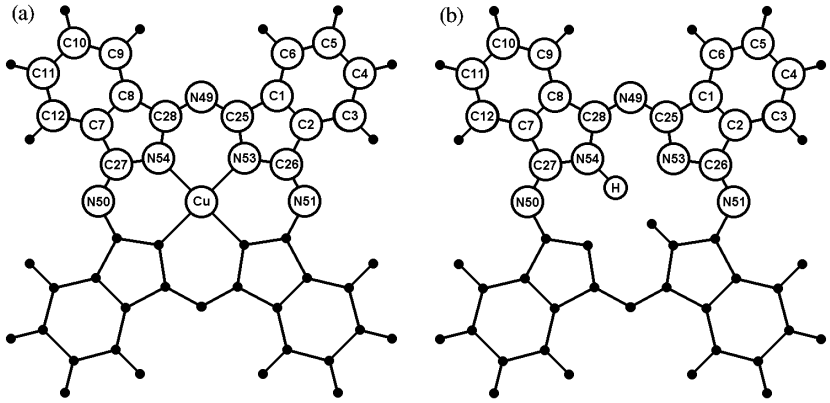

Figure 1. The molecular structures of (a) CuPc and (b) H_2Pc.

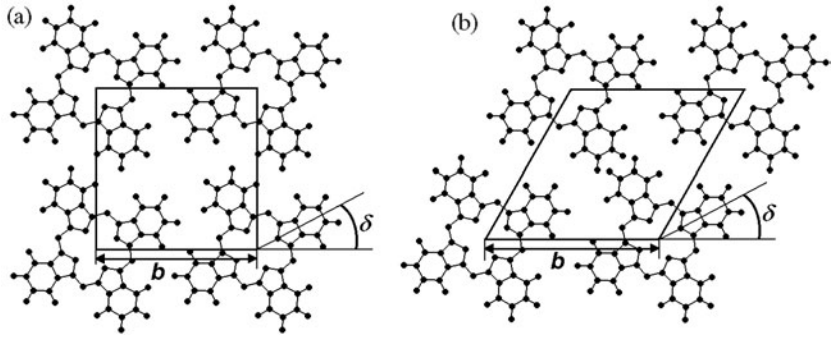

Figure 2. Schematic models of the (a) quadratic and (b) hexagonal 2D surface unit cells consisting of four Pc molecules (either CuPc or H_2Pc).

Table 1. MM2X atom types and vdW parameters used in this work (see [23]).

Atom	Atom type	R^* (Å)	ε (eV)
C1	37	4.00	0.003 47
C25	57	4.00	0.003 47
N49	38	3.60	0.006 94
N53	39	3.60	0.006 94
H(–C)	5	2.80	0.001 74
H(–N)	23	1.60	0.000 87
Cu[a]	—	3.60	0.008 02

[a] See [21].

the calculations and these are listed in table 2. These values are consistent with experimental x-ray diffraction data [27, 28]. Intermolecular interaction energies were then calculated for quadratic and hexagonal 2D surface unit cells comprising four CuPc or H_2Pc molecules. The unit cell dimension, b, was varied from 1.2 to 2.2 nm with an increment of 0.001 nm, and the molecular rotational angle, δ, was changed from 0° to 180° with an increment of 0.1° (figure 2). We have also determined the intermolecular interaction energies of several CuPc and H_2Pc unit cells with a dimension satisfying the commensurate relationship to the InSb(100), InAs(100) and InSb(111)A substrates. These are shown in figure 3.

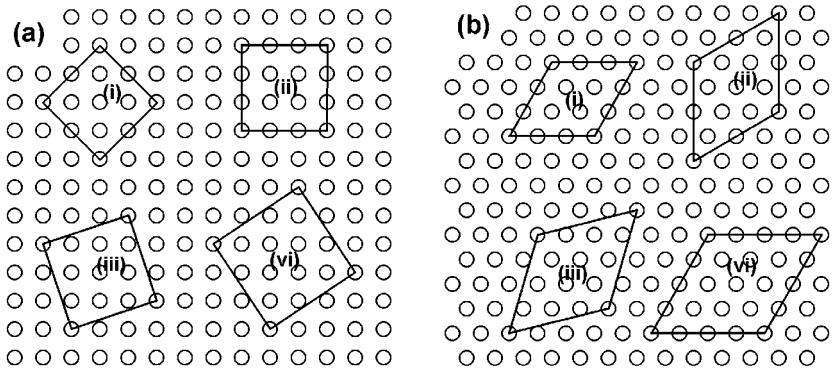

Figure 3. Schematic diagrams of several commensurate structures formed on (a) the (100) surface, (i) $(2\sqrt{2} \times 2\sqrt{2})$R45°, (ii) (3×3), (iii) $(\sqrt{10} \times \sqrt{10})$R ± 18.4° and (iv) $(\sqrt{13} \times \sqrt{13})$R ± 33.7°, and (b) the (111) surface, (i) (3×3), (ii) $(\sqrt{12} \times \sqrt{12})$R30°, (iii) $(\sqrt{13} \times \sqrt{13})$R ± 13.9° and (iv) (4×4).

4. Results

4.1. CuPc and H_2Pc deposition on the (100) surfaces of InSb and InAs

LEED patterns of the clean InAs(100) surface recorded with beam energies of 45 and 15 eV are shown in figures 4(a) and (b), respectively. Although there is some distortion of the pattern at 15 eV, it was important to record the diffraction patterns at low electron beam energies because of the large unit cells associated with the subsequently deposited organic overlayers. A $(4\times2)/c(8\times2)$ structure can be seen with a similar diffraction pattern obtained for InSb(100).

Deposition of CuPc leads to the formation of ordered overlayers on the InSb(100) and InAs(100) reconstructed surfaces. In each case the diffraction pattern associated with the clean surface reconstruction gradually fades and is replaced by the overlayer diffraction patterns presented in figures 4(c) and (e), both recorded at 15 eV beam energy. The patterns originate from CuPc molecules adopting a square lattice configuration. On InSb(100) (figure 4(c)) it is a simple (3×3) structure with lattice dimensions of 1.374 nm, whereas on InAs(100) (figure 4(e)) the pattern is generated by a square lattice in two domains, and a $(\sqrt{10} \times \sqrt{10})$R ± 18.4° structure is seen with lattice dimensions of 1.355 nm. Schematic diagrams of the reciprocal space structures seen in the LEED patterns are also shown in figures 4(d) and (f). The circles in figure 4(d) and the triangles in figure 4(f) indicate the (3×3) and $(\sqrt{10} \times \sqrt{10})$R ± 18.4° reciprocal space structures respectively, and the squares indicate substrate spots. The filled shapes represent the spots observed in the actual LEED patterns shown in figures 4(c) and (e). The reciprocal lattice unit cells associated with the adsorbate are indicated by solid line squares.

A LEED pattern of the clean InSb(100)-$(4 \times 2)/c(8 \times 2)$ surface recorded with a beam energy of 23 eV is shown in figure 5(a). Upon H_2Pc deposition the substrate spots gradually lose intensity and faint overlayer spots appear superimposed on the substrate pattern. Figure 5(b) shows the LEED pattern obtained at 13 eV after deposition of ∼1 ML of H_2Pc and this corresponds to a mixture of a (3×3) and $(\sqrt{10} \times \sqrt{10})$R ± 18.4° structure. A schematic diagram of the reciprocal space structure is shown in figure 5(d). The circles and triangles indicate the (3×3) and $(\sqrt{10} \times \sqrt{10})$R ± 18.4° reciprocal space structures respectively, and the squares indicate the substrate. The filled shapes represent the spots observed in the actual LEED pattern shown in figure 5(b). The (3×3) and $(\sqrt{10} \times \sqrt{10})$R ± 18.4° reciprocal lattice unit cells are indicated by the dashed and solid lines respectively. The LEED pattern

Table 2. Structural parameters of CuPc and H_2Pc obtained from *ab initio*/DFT calculations and x-ray diffraction studies (bond lengths are in Å and angles in degrees).

	CuPc		H_2Pc	
	Calculation[a]	X-ray[b]	Calculation[c]	X-ray[d]
C1–C2	1.397	1.400	1.404	1.396
C2–C3	1.385	1.388	1.393	1.388
C3–C4	1.385	1.388	1.397	1.386
C4–C5	1.398	1.415	1.405	1.392
C1–C25	1.443	1.453	1.467	1.459
C25–N53	1.367	1.366	1.365	1.369
C25–N49	1.315	1.326	1.336	1.328
C28–N49	1.315	1.326	1.318	1.328
C7–C8	1.397	1.400	1.414	1.397
C8–C9	1.385	1.388	1.397	1.392
C9–C10	1.385	1.388	1.392	1.382
C10–C11	1.398	1.415	1.410	1.398
C7–C27	1.443	1.453	1.453	1.454
C27–N54	1.367	1.366	1.378	1.372
C27–N50	1.315	1.326	1.318	1.323
$C–H_{av}$	1.086	—	1.086	—
N54–H			1.014	—
N–Cu	1.933	1.935		
C1–C2–C3	121.3	121.1	121.2	121.3
C2–C3–C4	117.5	117.9	117.7	117.3
C3–C4–C5	121.2	121.0	121.1	121.5
C1–C2–C26	106.5	106.0	105.6	106.5
C2–C26–N53	109.4	110.4	110.9	109.3
C25–N53–C26	108.2	107.3	106.9	108.6
N53–C26–N51	128.1	127.6	127.7	128.7
N49–C25–N53	128.1	127.6	127.6	128.7
C25–N49–C28	122.2	122.2	123.7	123.8
C7–C8–C9	121.3	121.1	120.9	121.2
C8–C9–C10	117.5	117.9	117.7	117.4
C9–C10–C11	121.2	121.0	121.2	121.9
C7–C8–C28	106.5	106.0	107.5	106.9
C8–C28–N54	109.4	110.4	106.1	108.4
C27–N54–C28	108.2	107.3	112.5	109.5
N54–C27–N50	128.1	127.6	128.2	126.9
N49–C28–N54	128.1	127.6	128.2	127.5
C28–N54–H			123.7	—
C28–N54–Cu	125.9	—		

[a] See [25].
[b] See [27].
[c] See [26].
[d] See [28].

associated with the overlayer becomes fainter with increasing coverage and the substrate spots rapidly disappear. The LEED pattern in figure 5(c) corresponds to ∼3 ML H_2Pc deposition. In real space, two different types of structure coexist: a (3×3) and a $(\sqrt{10} \times \sqrt{10})R \pm 18.4°$ structure. Each unit cell is quadratic and commensurate with unit cell dimensions of 1.374 and 1.449 nm respectively. The simultaneous existence of two commensurate domains with a quite different (∼0.075 nm) unit cell dimension implies a relatively strong substrate–molecule

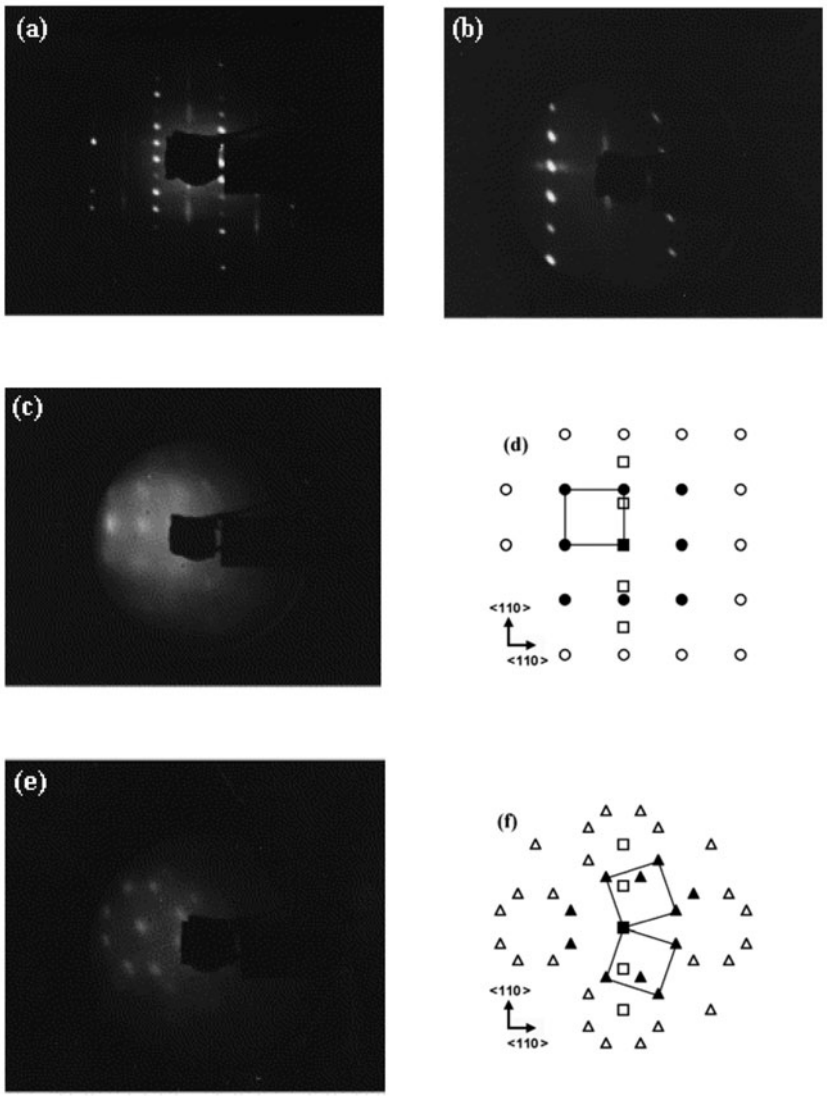

Figure 4. LEED patterns of (a), (b) clean InAs(100)-(4 × 2)/c(8 × 2), (c) ∼2 ML CuPc/InSb(100)-(4 × 2)/c(8 × 2) and (e) ∼2 ML CuPc/InAs(100)-(4 × 2)/c(8 × 2). The electron beam energies were (a) 45 eV, (b) 15 eV, (c) 15 eV and (e) 15 eV. Schematic diagrams of the reciprocal space structures are shown in (d) and (f). The squares represent the substrate spots, and the circles in (d) and triangles in (f) indicate the (3 × 3) and ($\sqrt{10} \times \sqrt{10}$)R ± 18.4° reciprocal space structures with the filled shapes indicating the spots observed in the LEED patterns shown in (c) and (e) respectively. The overlayer reciprocal lattice unit cells are indicated by the solid lines.

interaction since it means that the energy lowering achieved by epitaxy is more important than the energetic penalty associated with the change of intermolecular interaction. Annealing the adsorbate-covered surface resulted in a decrease in the intensity of the diffraction spots and an increase in the brightness of the screen background without any other apparent changes.

The same experiments were carried out with H_2Pc deposited on InAs(100); however, no ordered LEED patterns were observed for any deposition condition or after annealing.

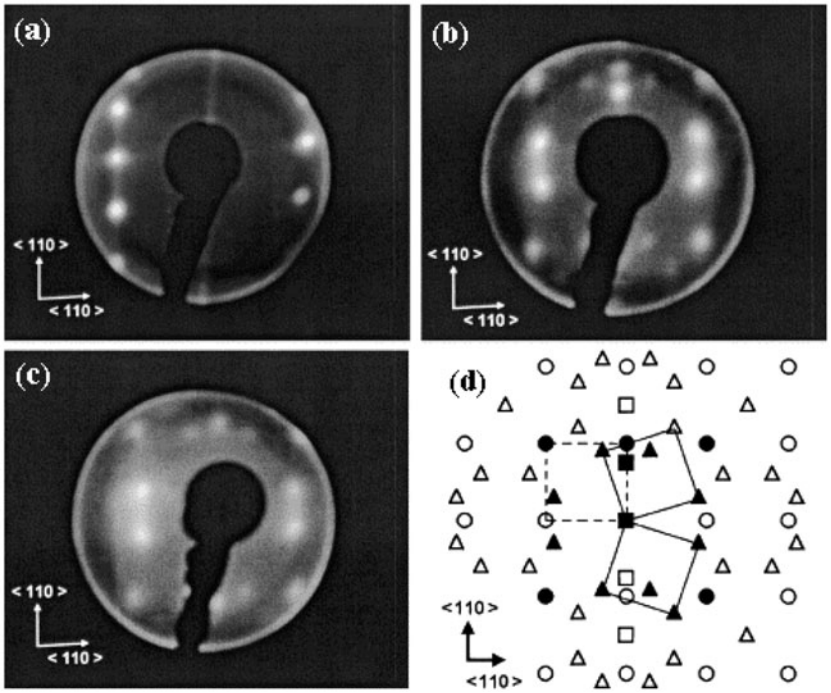

Figure 5. LEED patterns of (a) clean InSb(100)-(4 × 2)/c(8 × 2), (b) ∼1 ML H_2Pc/InSb(100)-(4 × 2)/c(8 × 2) and (c) ∼3 ML H_2Pc/InSb(100)-(4 × 2)/c(8 × 2). The electron beam energies were (a) 23 eV, (b) 13 eV and (c) 13 eV. A schematic of the reciprocal space structure is shown in (d). The squares represent the substrate spots, and the circles and triangles indicate the (3 × 3) and ($\sqrt{10} \times \sqrt{10}$)R ± 18.4° reciprocal space structures with the filled shapes indicating the spots observed in the LEED pattern shown in (b). The (3 × 3) and ($\sqrt{10} \times \sqrt{10}$)R ± 18.4° reciprocal lattice unit cells are indicated by the dashed and solid lines, respectively.

4.2. CuPc and H_2Pc deposition on InSb(111)A

The LEED patterns obtained from the (111)A surface of InSb, shown in figure 6(a), exhibited the well known (2×2) reconstruction that is generally interpreted in terms of an indium vacancy model with one vacancy per unit cell [29]. During the initial stages of CuPc deposition, the diffraction pattern associated with the clean surface is augmented by a faint array of additional spots which form a clear, sharp pattern as more CuPc is deposited, up to a coverage of about 2 ML. A typical LEED pattern is shown in figure 6(b) for 2 ML CuPc/InSb(111)A, recorded with an electron beam energy of 15 eV. The effect of multilayer deposition on the LEED pattern was a general loss of sharpness and increase in background intensity. Gentle annealing of the adsorbate-covered surface had no apparent effect on the quality of the diffraction patterns, although the sharpest pattern was obtained when CuPc was deposited at 100 °C. The diffraction pattern of the overlayer is generated by a diamond-shaped CuPc lattice with reciprocal space unit cell dimensions of $1/\sqrt{12}$ of the substrate lattice, rotated by 30° with respect to the substrate. A schematic diagram of the LEED pattern in reciprocal space is shown in figure 6(d). The reciprocal lattice unit cells of the (1 × 1) substrate and ($\sqrt{12} \times \sqrt{12}$)R30° overlayer are indicated by the dashed and solid lines, respectively. The filled circles represent the spots observed in the LEED pattern. In real space the CuPc molecules adopt a commensurate

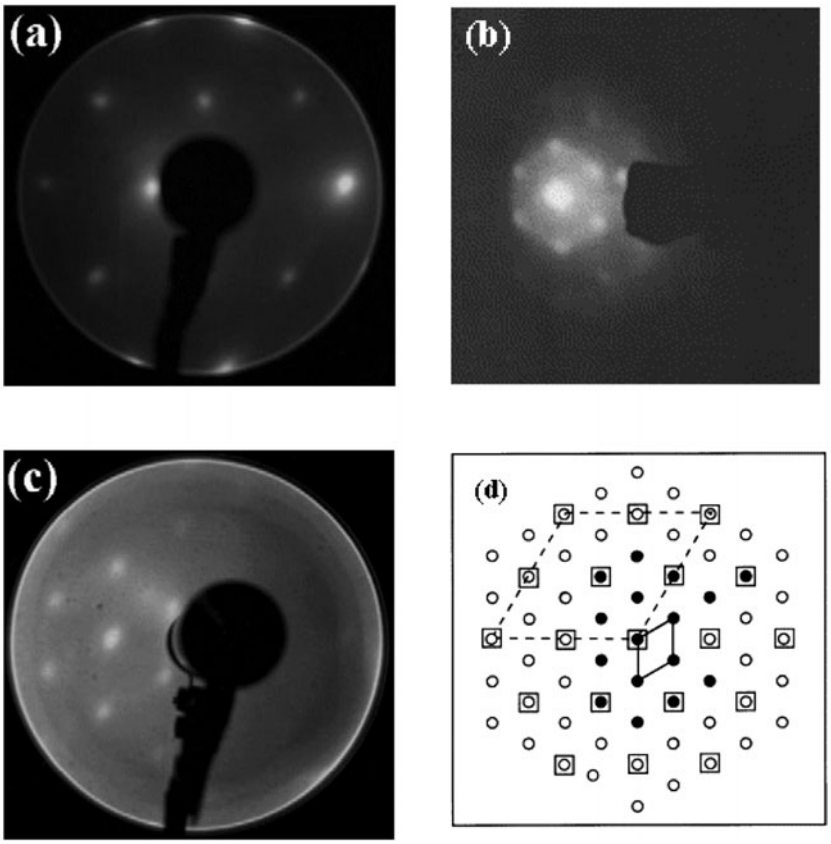

Figure 6. LEED patterns of (a) clean InSb(111)A-(2 × 2), (b) ∼2 ML CuPc/InSb(111)A-(2 × 2) and (c) ∼1 ML H_2Pc/InSb(111)A-(2 × 2). The electron beam energies were (a) 30 eV, (b) 15 eV and (c) 25 eV. A schematic diagram of the reciprocal space structure is shown in (d). The squares represent the substrate spots, and the circles indicate the ($\sqrt{12} \times \sqrt{12}$)R30° reciprocal space structures with the filled shapes indicating the spots observed in the LEED patterns. The reciprocal lattice unit cells of the substrate (1 × 1) and overlayer ($\sqrt{12} \times \sqrt{12}$)R30° are indicated by the dashed and solid lines, respectively.

($\sqrt{12} \times \sqrt{12}$)R30° structure on the InSb(111)A surface. The overlayer unit cell is hexagonal with a dimension of 1.587 nm and the included angle between the CuPc lattice unit vectors is 60°.

Deposition of H_2Pc onto InSb(111)A gives rise to similar diffraction patterns. Upon initial deposition of H_2Pc, the substrate (2 × 2) spots gradually disappear and a diffuse ring-shape diffraction feature appears. As deposition proceeds, this ring-shape feature diminishes and an ordered ($\sqrt{12} \times \sqrt{12}$)R30° pattern is obtained (figure 6(c)). The sharpest patterns were obtained when H_2Pc was deposited at 100 °C or annealed to 200 °C after room temperature deposition. This suggests that a more ordered structure is formed at higher temperature due to enhanced molecular lateral diffusion.

5. Discussion

It is somewhat surprising that ordered Pc structures are observed on unpassivated semiconductor surfaces, in particular when the presence of chemically active dangling bonds is

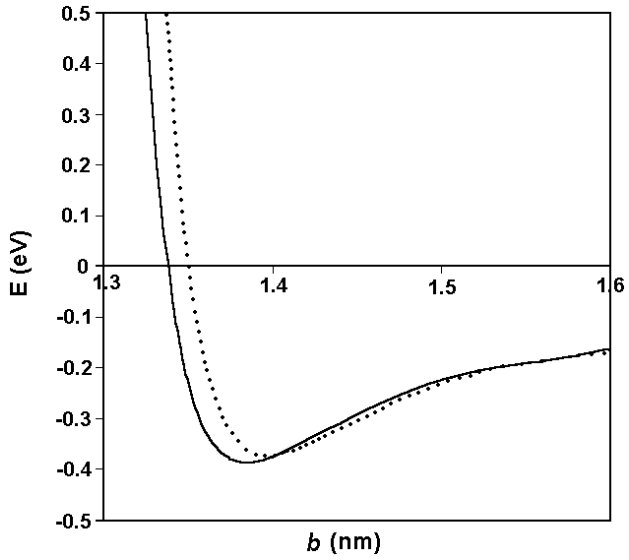

Figure 7. vdW intermolecular interaction energy curves for quadratic unit cells of CuPc (solid) and H_2Pc (dotted) with the unit cell dimension, b.

considered. Indeed, our results indicate that the substrate–molecule interaction must be weak enough to allow sufficient lateral diffusion of the molecules across the surface to produce ordered structures.

To gain greater insight into the structural differences that occur when CuPc and H_2Pc are deposited on InSb(100) and InAs(100), the calculated vdW intermolecular interaction energies for the quadratic unit cells of the two molecules are compared with the actual structures observed by the LEED results. For calculations, all four molecules in the unit cell are assumed to lie parallel to the surface, a reasonable assumption since previous studies using RAIRS [30] and STM [9, 31–33] support a flat-lying orientation for a quadratic 2D Pc layer on substrates with a sufficiently strong substrate–molecule interaction. Furthermore, our own recent studies of H_2Pc/InSb(100) using high-resolution electron energy loss spectroscopy (HREELS) suggest that the initial layers of molecules are aligned essentially parallel to the substrate.

The vdW interaction energy curves for the quadratic unit cells of CuPc (solid) and H_2Pc (dotted) are shown in figure 7 with respect to the lattice dimension, b. At each value of b, the energy is the value determined at δ, the molecular rotational angle, to maintain the minimum energy. The CuPc unit cell has a minimum energy of -0.39 eV at $b = 1.385$ nm and $\delta = 27.3°$, and the H_2Pc unit cell has a minimum energy of -0.37 eV at $b = 1.397$ nm and $\delta = 27.4°$. Comparison of the intermolecular interaction energies at several possible commensurate lattice dimensions can quantitatively rationalize the structural variation of the Pc layers grown on the (100) surfaces of InSb and InAs (table 3).

The LEED studies reported in section 4 show that CuPc forms a (3×3) structure on InSb(100) and a $(\sqrt{10} \times \sqrt{10})R \pm 18.4°$ structure on InAs(100). The calculated intermolecular interaction energy for a (3×3) CuPc unit cell on InSb(100) is -0.38 eV at $b = 1.374$ nm. In the case of the $(2\sqrt{2} \times 2\sqrt{2})R45°$ structure at $b = 1.296$ nm the energy is 4.79 eV, whilst for the $(\sqrt{10} \times \sqrt{10})R \pm 18.4°$ structure at $b = 1.449$ nm it is -0.29 eV. These last two values are 5.15 and 0.09 eV higher than that of the (3×3) structure. For CuPc on InAs(100), the intermolecular interaction energy has a value of -0.28 eV for the $(\sqrt{10} \times \sqrt{10})R \pm 18.4°$ unit

Table 3. vdW interaction energy minima of the CuPc and H_2Pc quadratic unit cells at several lattice dimensions which are commensurate to the (100) surfaces of InSb and InAs.

	CuPc			H_2Pc		
	b (nm)	δ (deg)	E (eV)	b (nm)	δ (deg)	E (eV)
Minimum E	1.385	27.3	−0.39	1.397	27.4	−0.37
InSb(100)						
$(2\sqrt{2} \times 2\sqrt{2})R \pm 45°$	1.296	62.0	4.79	1.296	61.7	9.19
(3×3)	1.374	27.4	−0.38	1.374	27.6	−0.32
$(\sqrt{10} \times \sqrt{10})R \pm 18.4°$	1.449	25.5	−0.29	1.449	25.8	−0.31
$(\sqrt{13} \times \sqrt{13})R \pm 33.7°$	1.652	16.6	−0.13	1.652	16.8	−0.13
InAs(100)						
(3×3)	1.285	61.9	9.26	1.285	61.6	16.90
$(\sqrt{10} \times \sqrt{10})R \pm 18.4°$	1.355	27.5	−0.28	1.355	27.8	−0.09
$(\sqrt{13} \times \sqrt{13})R \pm 33.7°$	1.545	69.7	−0.19	1.545	68.6	−0.19

cell structure at $b = 1.355$ nm, whilst the energy of the (3×3) structure at $b = 1.285$ nm is 9.26 eV and that of the $(\sqrt{13} \times \sqrt{13})R \pm 33.7°$ structure at $b = 1.545$ nm is −0.19 eV. These two values are 9.54 and 0.09 eV higher than that of the $(\sqrt{10} \times \sqrt{10})R \pm 18.4°$ structure. These comparisons suggest that the (3×3) and the $(\sqrt{10} \times \sqrt{10})R \pm 18.4°$ unit cells of CuPc are favourable commensurate structures on InSb(100) and InAs(100) respectively, since they minimize the penalty of the intermolecular interaction energy arising from deviation for the bulk molecular structures. In the case of H_2Pc on InSb(100), however, the intermolecular interaction energies for the (3×3) and $(\sqrt{10}\times\sqrt{10})R\pm18.4°$ structure are essentially identical with values of −0.32 and −0.31 eV respectively. This is consistent with the observed LEED pattern which shows the presence of both types of unit cell structure (figure 5).

The calculated intermolecular interaction energies for the $(\sqrt{10} \times \sqrt{10})R \pm 18.4°$ and $(\sqrt{13} \times \sqrt{13})R \pm 33.7°$ unit cells on InAs(100) are −0.09 and −0.19 eV respectively. From the viewpoint of the intermolecular interaction energy, the $(\sqrt{13} \times \sqrt{13})R \pm 33.7°$ is the most favourable commensurate structure for H_2Pc on InAs(100). One possible explanation for the absence of any LEED pattern in this system is that the penalty of the intermolecular interaction energy required to maintain the commensurate structure is quite high (0.18 eV) when compared with CuPc on InSb (0.01 eV) and InAs (0.10 eV), and H_2Pc on InSb (0.05–0.06 eV). Unfortunately it is impossible to quantify this effect since the strength of the substrate–molecule interaction is unknown.

Real space structures expected from the diffraction patterns and intermolecular interaction energy calculations are shown schematically in figure 8. The exact lattice sites over which the CuPc and H_2Pc molecules are positioned are not known. All diagrams show the ideal terminated surface (non-reconstructed) with which the CuPc and H_2Pc overlayers are commensurate. The projection of each molecule points into the hollows of its neighbours, the so-called 'dovetail' principle, as this type of packing has been observed by STM in previous studies of flat-lying Pc molecules [34, 35]. The calculations rationalize the existence of the dovetail structure as a consequence of the minimization of the intermolecular interaction energy for Pc molecules in their respective lattice.

Ordered Pc structures are also obtained on the InSb(111)A-(2×2) surface, with CuPc and H_2Pc both forming a hexagonal, commensurate $(\sqrt{12} \times \sqrt{12})R30°$ structure. The hexagonal structure is very different to any structure that has been identified for vapour deposition of Pcs onto any substrate type. The identification of hexagonal Pc structures implies that substrate–

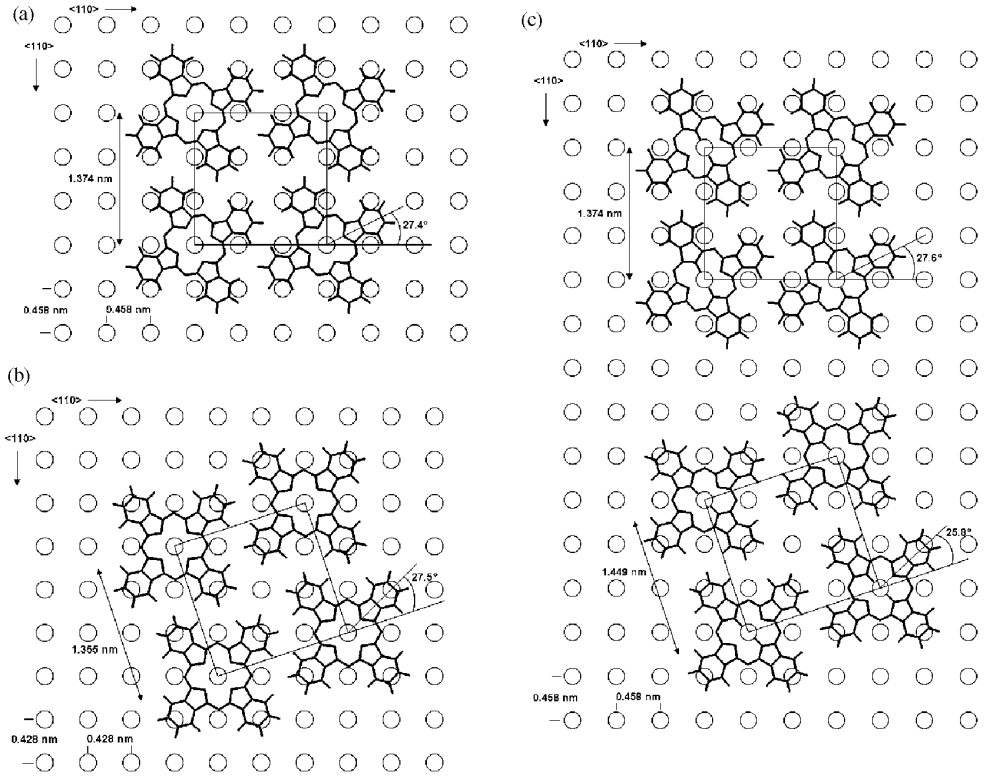

Figure 8. The proposed structures of (a) CuPc deposited on InSb(100), (b) CuPc deposited on InAs(100) and (c) H_2Pc deposited on InSb(100). The structures are drawn with respect to the ideal terminated surfaces. The squares represent the surface unit meshes. The exact sites over which the CuPc and H_2Pc molecules are positioned are not known.

molecule interactions appear to dominate over intermolecular interactions, since intermolecular interactions would preferentially lead to a quadratic or nearly quadratic lattice. It is surprising that a $(\sqrt{12} \times \sqrt{12})$R30° structure is adopted for deposition on InSb(111)A, particularly when the intermolecular separation which results from such a structure is considered. The intermolecular spacing of the Pc unit cell on InSb(111)A is 1.59 nm, ∼15% larger than the usual CuPc and H_2Pc intermolecular spacing of 1.37–1.40 nm which have been reported for deposition on a variety of layered materials and ionic surfaces [6]. The unit cell area of the Pc structure on InSb(111)A is also ∼14% larger than the quadratic unit cells reported so far. This large intermolecular spacing can, however, be explained using intermolecular interaction energy calculations of the hexagonal Pc unit cells.

The vdW intermolecular interaction energy curves for the hexagonal unit cells of CuPc (solid black) and H_2Pc (dotted black) are shown in figures 9(a) and (b) respectively, with respect to the lattice dimension, b. As before, the energy at each point of b is the value determined at δ, the molecular rotational angle, to maintain the minimum energy. The CuPc unit cell has a minimum energy of −0.13 eV at $b = 1.666$ nm and $\delta = 45.0°$, and the H_2Pc unit cell has a minimum energy of −0.13 eV at $b = 1.677$ nm and $\delta = 45.0°$. In the case of hexagonal CuPc and H_2Pc unit cells, the lattice dimensions at the energy minima are 20.3 and 20.0% larger respectively than the quadratic unit cell lattice dimensions. The

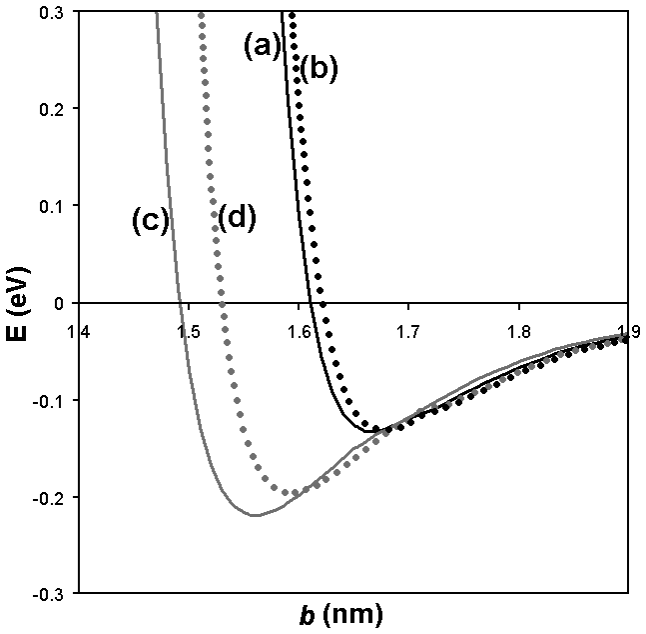

Figure 9. vdW intermolecular interaction energy curves for hexagonal unit cells of (a) CuPc at $\tau = 0°$, (b) H_2Pc at $\tau = 0°$, (c) CuPc at $\tau = 7°$ and (d) H_2Pc at $\tau = 7°$ with respect to the unit cell dimension, b.

calculations show that, for quadratic unit cells, the repulsive energy can be minimized by adopting the dovetail structure since Pc molecules have fourfold or nearly fourfold symmetry. The hexagonal unit cell, however, cannot have such a dovetail structure and, with the small unit cell dimension, the repulsion between the close diagonal molecules is unavoidable. The intermolecular interaction energy minimum for the CuPc and H_2Pc hexagonal unit cells is -0.13 eV. This higher PE minimum indicates that the hexagonal structure is less favourable than a quadratic unit cell in terms of the intermolecular interaction energy. Nevertheless, the identification of hexagonal structures in the LEED studies implies a reasonably strong substrate–molecule interaction between the Pc molecules and the InSb(111)A surface.

Among the potential hexagonal commensurate structures shown in figure 3(b), the $(\sqrt{13} \times \sqrt{13})R \pm 13.9°$ is the most energetically favourable. The intermolecular interaction energy for the $(\sqrt{13} \times \sqrt{13})R \pm 13.9°$ hexagonal unit cell is -0.13 eV at $\delta = 45.0°$ for CuPc, and -0.11 eV at $\delta = 45.0°$ for H_2Pc, values which are 0.38 and 0.52 eV lower than the energy of the $(\sqrt{12} \times \sqrt{12})R30°$ structures. The energetically unfavourable hexagonal structure and lattice dimensions are thought to be related to the existence of In vacancies in the underlying (2×2) reconstructed surface. Real space $(\sqrt{12} \times \sqrt{12})R30°$ structures expected from the diffraction patterns and intermolecular interaction energy calculations are shown in figure 10. In contrast to the models drawn for the growth on the (100) surfaces, the Pc structures in figure 10 are drawn with respect to the (2×2) reconstructed InSb(111)A surface, with the molecules centred on the In vacancy sites although the exact adsorption sites are unknown. We speculate, therefore, that although Pc molecules interact weakly with surface In atoms and are able to undergo lateral diffusion, they have a relatively strong interaction with the second layer Sb atoms that are exposed because of the existence of In vacancies in the (2×2) reconstructed surface. Additional experimental studies will be required to verify the adsorption site and molecule–surface interaction.

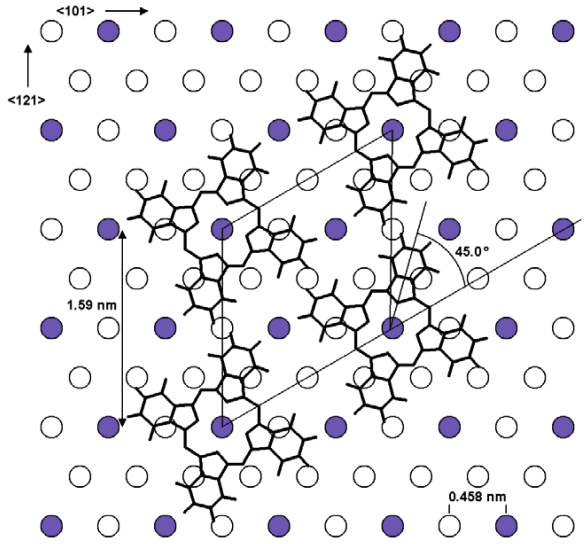

Figure 10. The proposed structures for Pcs deposited on InSb(111)A-(2 × 2). Only one domain is drawn for clarity and the structure is drawn with respect to the (2 × 2) reconstructed surface with indium vacancies. The solid line represents the adsorbate unit cell and filled circles indicate the In vacancies. The exact sites over which the Pc molecules are positioned are not known.

(This figure is in colour only in the electronic version)

One possible way in which the vdW repulsions are reduced in a unit cell with small lattice dimensions is through tilting of the Pc molecules. In fact, there has been a report of tilted CuPc molecules on the unpassivated Si(111) surface [36], with STM studies indicating a tilt angle, τ, with respect to the surface plane, of 27°. Intermolecular interaction energy calculations that include tilting can have a dramatic effect on the PE minima and the lattice dimensions of the 2D unit cells. Energy curves for the hexagonal CuPc (solid grey) and H_2Pc (dotted grey) unit cells at $\tau = 7°$ are drawn in figures 9(c) and (d) respectively. The CuPc unit cell has a minimum energy of -0.22 eV at $b = 1.560$ nm and $\delta = 45.0°$, and the H_2Pc unit cell has a minimum energy of -0.20 eV at $b = 1.593$ nm and $\delta = 42.8°$. The minimum energies at several commensurate lattice dimensions with two different tilt angles, $\tau = 0°$ and 7°, are listed in table 4. Clearly, additional experimental studies are required using techniques such as STM in order to rationalize the existence of energetically unfavourable Pc structures on InSb(111)A.

6. Conclusion

Ordered CuPc and H_2Pc structures are formed on unpassivated, In-terminated InSb(100)-(4 × 2)/c(8 × 2) and InSb(111)A-(2 × 2) reconstructed surfaces, with an ordered CuPc structure also formed on InAs(100)-(4 × 2)/c(8 × 2). The structure formed is influenced by the orientation and lattice dimensions of the substrates. CuPc forms a single-domain (3 × 3) structure on InSb(100) and a ($\sqrt{10} \times \sqrt{10}$)R ± 18.4° structure on InAs(100). By contrast, H_2Pc forms a mixed (3 × 3) and ($\sqrt{10} \times \sqrt{10}$)R ± 18.4° structure on InSb(100), but no ordered overlayer structure is adopted on InAs(100). These structural differences have been rationalized by theoretical calculations of the vdW intermolecular interaction energies. The calculations take into account the unit cell dimensions and the molecular rotational angle of

Table 4. vdW interaction energy minima of the CuPc and H_2Pc hexagonal unit cells with different molecular tilt angles, $\tau = 0°$ and 7°, at several lattice dimensions which are commensurate to the InSb(111)A surface.

	CuPc			H_2Pc		
	b (nm)	δ (deg)	E (eV)	b (nm)	δ (deg)	E (eV)
at $\tau = 0°$						
Minimum E	1.666	45.0	−0.13	1.677	45.0	−0.13
(3×3)	1.374	78.8	$>10^3$	1.374	79.9	$>10^3$
$(\sqrt{12} \times \sqrt{12})$R30°	1.587	45.0	0.25	1.587	45.0	0.41
$(\sqrt{13} \times \sqrt{13})$R ± 13.9°	1.652	45.0	−0.13	1.652	45.0	−0.11
(4×4)	1.832	30.0	−0.05	1.832	30.0	−0.06
at $\tau = 7°$						
Minimum E	1.560	45.0	−0.22	1.593	42.8	−0.20
(3×3)	1.374	45.0	13.3	1.374	22.0	17.8
$(\sqrt{12} \times \sqrt{12})$R30°	1.587	45.0	−0.21	1.587	42.8	−0.20
$(\sqrt{13} \times \sqrt{13})$R ± 13.9°	1.652	45.0	−0.15	1.652	43.0	−0.16
(4×4)	1.832	28.5	−0.05	1.832	60.0	−0.06

the molecules. CuPc on InSb(100) has a minimum energy when the structure is (3×3), whereas on InAs(100) the minimum energy accounts for the $(\sqrt{10} \times \sqrt{10})$R ± 18.4° structure. In the case of H_2Pc on InSb(100), the energies of the (3×3) and $(\sqrt{10} \times \sqrt{10})$R ± 18.4° structures are equivalent. For H_2Pc on InAs(100), the lack of any ordered LEED pattern can be rationalized by the penalty of the intermolecular interaction energy in maintaining a commensurate overlayer structure.

On InSb(111)A CuPc and H_2Pc both form a $(\sqrt{12} \times \sqrt{12})$R30° structure, which is hexagonal and commensurate with a lattice dimension of 1.59 nm. The identification of this hexagonal Pc structure which is energetically less favourable than a quadratic structure implies the existence of a relatively strong substrate–molecule interaction between the Pc molecules and the InSb(111)A surface. The observed $(\sqrt{12} \times \sqrt{12})$R30° structure does not coincide exactly with the calculated intermolecular interaction energy minimum; the existence of In vacancies on the (2×2) reconstructed surface and the possibility of molecular tilting may be responsible for the existence of this unusual Pc structure.

Acknowledgments

SY is grateful for a scholarship from the Overseas Research Student (ORS) Awards. The Engineering and Physical Sciences Research Council (EPSRC), UK is acknowledged for financial support through contract number GR/M 54285.

References

[1] See for example Forrest S R 1997 *Chem. Rev.* **97** 1793 and references therein
[2] Wang D W, Tanaka Y, Iizuka M, Kuniyoshi S, Kudo S and Tanaka K 1999 *Japan. J. Appl. Phys.* **38** 256
[3] Gu G, Khalfin V and Forrest S R 1998 *Appl. Phys. Lett.* **73** 2399
[4] van Slyke S A, Chen C H and Tang C W 1996 *Appl. Phys. Lett.* **69** 2160
[5] Hook D E, Fritz T and Ward M D 2001 *Adv. Mater.* **13** 227
[6] Koma A 1995 *Prog. Cryst. Growth Charact.* **30** 129
[7] Ludwig C, Gompf B, Petersen J, Eisenmenger W, Möbus M, Zimmermann U and Karl N 1992 *Z. Phys.* B **86** 397

[8] Ludwig C, Gompf B, Petersen J, Stromaier R and Eisenmenger W 1994 *Z. Phys.* B **93** 365
[9] Schuerlein T J and Armstrong N R 1994 *J. Vac. Sci. Technol.* A **12** 1992
[10] Buchholz J C and Somorjai G A 1977 *J. Chem. Phys.* **66** 573
[11] Rochet F, Dufour G, Roulet H, Motta N, Sgarlata A, Piancastelli M N and De Crescenzi M 1994 *Surf. Sci.* **319** 10
[12] Umbach E, Sokolowski M and Fink P 1996 *Appl. Phys.* A **63** 565
[13] Tada H, Kawaguchi T and Koma A 1992 *Appl. Phys. Lett.* **61** 2021
[14] Hirose Y, Forrest S R and Kahn A 1995 *Appl. Phys. Lett.* **66** 944
[15] Yamamoto H, Tada H, Kawaguchi T and Koma A 1994 *Appl. Phys. Lett.* **64** 2099
[16] Hirose Y, Forrest S R and Kahn A 1995 *Phys. Rev.* B **52** 14040
[17] Kendrick C and Kahn A 1997 *J. Cryst. Growth* **181** 181
[18] Cox J J and Jones T S 2000 *Surf. Sci.* **457** 311
[19] Yim S and Jones T S 2002 *Surf. Sci.* **521** 151
[20] Forrest S R and Zhang Y 1994 *Phys. Rev.* B **49** 11297
[21] Nakamura M and Tokumoto H 1998 *Surf. Sci.* **398** 143
[22] Bell G R, McConville C F and Jones T S 1996 *Appl. Surf. Sci.* **104/105** 17
[23] Halgren T A 1992 *J. Am. Chem. Soc.* **114** 7827
[24] Yim S, Heutz S and Jones T S 2003 *Phys. Rev.* B **67** 165308
[25] Mastryukov V, Ruan C, Fink M, Wang Z and Pachter R 2000 *J. Mol. Struct.* **556** 225
[26] Gong X D, Xiao H M and Tian H 2002 *Int. J. Quantum Chem.* **86** 531
[27] Brown C J 1968 *J. Chem. Soc.* A 2488
[28] Zugenmaier P, Bluhm T L, Deslandes Y, Orts W J and Hamer G K 1997 *J. Mater. Sci.* **32** 5561
[29] Duke C B 1993 *J. Vac. Sci. Technol.* B **11** 1336
[30] Tokito S, Sakata J and Taga Y 1995 *Thin Solid Films* **256** 182
[31] Lippel P H, Wilson R J, Miller M D, Wöll Ch and Chiang S 1989 *Phys. Rev. Lett.* **62** 171
[32] Maeda Y, Matsumoto T, Kasaya M and Kawai T 1996 *Japan. J. Appl. Phys.* **35** L405
[33] Kanai M, Kawai T, Motai K, Wang X D, Hashizume T and Sakura T 1995 *Surf. Sci.* **329** L619
[34] Ludwig C, Strohmaier R, Petersen J, Gompf B and Eisenmenger W 1994 *J. Vac. Sci. Technol.* B **12** 1963
[35] Lu X, Hipps K W, Wang X D and Mazur U 1996 *J. Am. Chem. Soc.* **118** 7197
[36] Hiesgen R, Rabisch M, Bottcher H and Meissner D 2000 *Sol. Energy Mater. Sol. Cells* **61** 73
[37] Upward M D, Beton P H and Moriarty P 1999 *Surf. Sci.* **441** 21